

TMA4220 - PROJECT 2

OTTAR HELLAN, JOHANNES VOLL KOLSTØ AND GJERMUND LYCKANDER

CONTENTS

1. Introduction	1
2. Theory	1
2.1. Linear Elasticity	1
2.2. Governing Equation	2
2.3. Variational Form	2
2.4. Discretization	4
2.5. Periodic Solutions	5
3. Implementation	5
3.1. Convergence in the L^2 norm	5
4. Numerical Experiments	7
4.1. Vibration frequencies	8
5. Discussion	9
6. Conclusion	10
References	11
Appendix	11
A: Verify Analytical Solution	11
B: Plate Triangulation	13

1. INTRODUCTION

In this report we perform vibrational analysis on plates of different materials in two dimensions using the Finite Element Method (FEM). A solver made for the Poisson problem is adapted to solve the linear elasticity equation and we use the resulting mass and stiffness matrices to solve the generalized eigenvalue problem giving the free vibrations of the plates. The vibrations in uniform plates of stainless steel, aluminium, and timber are compared and the resulting vibrations are found to be qualitatively largely equivalent.

2. THEORY

2.1. Linear Elasticity. The three main elements of linear elasticity are the *displacement* \mathbf{u} , the *strain* $\boldsymbol{\varepsilon}$ and the *stress* $\boldsymbol{\sigma}$.

$$\mathbf{u} = \begin{bmatrix} u_x \\ u_y \end{bmatrix}, \quad \boldsymbol{\varepsilon} = \begin{bmatrix} \varepsilon_{xx} & \varepsilon_{xy} \\ \varepsilon_{xy} & \varepsilon_{yy} \end{bmatrix}, \quad \boldsymbol{\sigma} = \begin{bmatrix} \sigma_{xx} & \sigma_{xy} \\ \sigma_{xy} & \sigma_{yy} \end{bmatrix}$$

TABLE 1. Definitions of the different elements in our linear elasticity problem.

The subscripts denote vector components, not derivatives. The displacement vector \mathbf{u} is a measure of how the material in our domain has moved in each dimension. The strain tensor $\boldsymbol{\varepsilon}$ is a measure of how much a line segment has stretched or deformed relative to its original length. As long as the stretching is small, the relation between $\boldsymbol{\varepsilon}$ and \mathbf{u} can be linearized, leading to a more tractable problem. The stress tensor $\boldsymbol{\sigma}$ is a measure of how much force the nodal point experiences per area.

The three main variables can be expressed as functions of position and each other,

$$\mathbf{u} = \mathbf{u}(\mathbf{x}), \quad \boldsymbol{\varepsilon} = \boldsymbol{\varepsilon}(\mathbf{u}), \quad \boldsymbol{\sigma} = \boldsymbol{\sigma}(\boldsymbol{\varepsilon}).$$

If we imagine an object with a line segment in the x -direction of original length α and stretched length α' , the strain of the segment is defined as $\varepsilon_{xx} = \frac{\alpha' - \alpha}{\alpha}$. From this the following relations can be derived:

$$\varepsilon_{xx}(\mathbf{u}) = \frac{\partial u_x}{\partial x}, \quad \varepsilon_{yy}(\mathbf{u}) = \frac{\partial u_y}{\partial y}, \quad \varepsilon_{xy}(\mathbf{u}) = \frac{\partial u_x}{\partial y} + \frac{\partial u_y}{\partial x}.$$

The relationship between $\boldsymbol{\varepsilon}$ and $\boldsymbol{\sigma}$ is taken from the project description and can be expressed as:

$$(2.1) \quad \boldsymbol{\sigma} = C\boldsymbol{\varepsilon}$$

$$\begin{bmatrix} \sigma_{xx} \\ \sigma_{yy} \\ \sigma_{xy} \end{bmatrix} = \frac{E}{1 - \nu^2} \begin{bmatrix} 1 & \nu & 0 \\ \nu & 1 & 0 \\ 0 & 0 & \frac{1-\nu}{2} \end{bmatrix} \begin{bmatrix} \varepsilon_{xx} \\ \varepsilon_{yy} \\ \varepsilon_{xy} \end{bmatrix}$$

Here E is the Young's modulus of the material and ν is the ratio of compression vs expansion, known as the Poisson's ratio.

2.2. Governing Equation. The governing equation for our system is Newton's second law in two dimensions, accounting for stress forces $\boldsymbol{\sigma}$ induced by strain in the 2D material, along with tangential surface forces \mathbf{f} ,

$$(2.2) \quad \rho \ddot{\mathbf{u}} = \nabla \boldsymbol{\sigma}(\mathbf{u}) + \mathbf{f}, \quad (x, y) \in \Omega.$$

Here the dots represent time derivatives, and ρ is the density per area of our material.

For an object at static equilibrium the time derivatives go to zero and we get the problem formulation

$$\nabla \boldsymbol{\sigma}(\mathbf{u}) = -\mathbf{f}$$

$$\left[\frac{\partial}{\partial x}, \quad \frac{\partial}{\partial y} \right] \begin{bmatrix} \sigma_{xx} & \sigma_{xy} \\ \sigma_{xy} & \sigma_{yy} \end{bmatrix} = -[f_x, f_y],$$

with the following boundary conditions on $\partial\Omega_D \cup \partial\Omega_N = \partial\Omega$, and $\text{int } \Omega_D \cap \text{int } \partial\Omega_N = \emptyset$:

$$\begin{aligned} \mathbf{u} &= \mathbf{g}, \quad \text{for } \mathbf{u} \in \partial\Omega_D, \\ \boldsymbol{\sigma} \cdot \hat{\mathbf{n}} &= \mathbf{h}, \quad \text{for } \mathbf{u} \in \partial\Omega_N. \end{aligned}$$

2.3. Variational Form. Multiplying with the test function $\mathbf{v} = \begin{bmatrix} v_1(x, y) \\ v_2(x, y) \end{bmatrix}$ and integrating over the domain Ω we get

$$(2.3) \quad \int_{\Omega} \nabla^T \boldsymbol{\sigma}(\mathbf{u}) \mathbf{v} dA = - \int_{\Omega} \mathbf{f}^T \mathbf{v} dA.$$

The left-hand side of (2.3) can be written as

$$\int_{\Omega} \nabla^T \boldsymbol{\sigma}(\mathbf{u}) \mathbf{v} dA = \sum_{ij=xx,xy,yx,yy} \int_{\Omega} \left(\frac{\partial \sigma_{ji}(u)}{\partial i} \right) v_j dA.$$

Using integration by parts we see that we end up with two terms, one boundary integral, and one over the entire domain Ω , as is typical for variational problem formulations.

$$\int_{\Omega} \left(\frac{\partial \sigma_{ji}(u)}{\partial i} \right) v_j dA = v_j \sigma_{ji} \hat{n}_i \Big|_{\partial\Omega} - \int_{\Omega} \sigma_{ji} \left(\frac{\partial}{\partial i} v_j \right) dA.$$

Furthermore we have that the integral over the domain Ω can be expressed in vector-matrix notation as

$$\begin{aligned} \sum_{ij=xx,xy,yx,yy} \int_{\Omega} \sigma_{ji} \left(\frac{\partial}{\partial i} v_j \right) dA &= \int_{\Omega} \left[\sigma_{xx} \left(\frac{\partial}{\partial x} v_x \right) + \sigma_{xy} \left(\frac{\partial}{\partial x} v_y \right) + \sigma_{xy} \left(\frac{\partial}{\partial y} v_x \right) + \sigma_{yy} \left(\frac{\partial}{\partial y} v_y \right) \right] dA, \\ &= \int_{\Omega} \left[\frac{\partial}{\partial x} v_x, \quad \frac{\partial}{\partial x} v_y + \frac{\partial}{\partial y} v_x, \quad \frac{\partial}{\partial y} v_y \right] \begin{bmatrix} \sigma_{xx} \\ \sigma_{xy} \\ \sigma_{yy} \end{bmatrix} dA, \\ &= \int_{\Omega} \boldsymbol{\varepsilon}(\mathbf{v})^T \boldsymbol{\sigma} dA = \sum_{ij=xx,xy,yy} \int_{\Omega} \varepsilon_{ij}(\mathbf{v}) \sigma_{ij}(\mathbf{u}) dA \end{aligned}$$

And for the boundary integral term over $\partial\Omega$

$$v_j \sigma_{ji} \hat{n}_i \Big|_{\partial\Omega} = \int_{\partial\Omega} \mathbf{v}^T \boldsymbol{\sigma}(\mathbf{u}) \hat{\mathbf{n}} dS = \sum_{i=x,y} \sum_{j=x,y} \int_{\partial\Omega} v_i \sigma_{ij} n_j dS$$

The right-hand side can be written as

$$(2.4) \quad \int_{\Omega} -\mathbf{f}^T \mathbf{v} dA = \sum_{i=1}^2 \int_{\Omega} -f_i v_i dA.$$

By now changing the subscripts (x, y) with $(1, 2)$ and using the derived equalities we obtain the scalar equation

$$(2.5) \quad \sum_{ij=xx,xy,yy} \int_{\Omega} \varepsilon_{ij}(\mathbf{v}) \sigma_{ij}(\mathbf{u}) dA = \sum_{i=1}^2 \int_{\Omega} f_i v_i dA + \sum_{i=1}^2 \sum_{j=1}^2 \int_{\partial\Omega} v_i \sigma_{ij} n_j dS.$$

If we now insert (2.1) into the left hand side of (2.5) we see that

$$(2.6) \quad \sum_{ij=xx,xy,yy} \int_{\Omega} \varepsilon_{ij}(\mathbf{v}) \sigma_{ij}(\mathbf{u}) dA = \int_{\Omega} \boldsymbol{\varepsilon}(\mathbf{v})^T \boldsymbol{\sigma} dA = \int_{\Omega} \boldsymbol{\varepsilon}(\mathbf{v})^T C \boldsymbol{\varepsilon}(\mathbf{u}) dA.$$

For the right hand side we see that for the boundary integral term we get

$$(2.7) \quad \sum_{i=1}^2 \sum_{j=1}^2 \int_{\partial\Omega} v_i \sigma_{ij} n_j dS = \int_{\partial\Omega} \mathbf{v}^T \boldsymbol{\sigma}(\mathbf{u}) \hat{\mathbf{n}} dS$$

$$(2.8) \quad = \int_{\partial\Omega_D} \mathbf{v}^T \boldsymbol{\sigma}(\mathbf{u}) \hat{\mathbf{n}} dS + \int_{\partial\Omega_N} \mathbf{v}^T \mathbf{h} dS.$$

Now rewriting (2.5) by using (2.4), (2.6) and (2.7) we get that the scalar equation can be written in compact vector form:

$$\int_{\Omega} \boldsymbol{\varepsilon}(\mathbf{v})^T C \boldsymbol{\varepsilon}(\mathbf{u}) dA = \int_{\Omega} \mathbf{f}^T \mathbf{v} dA + \int_{\partial\Omega_D} \mathbf{v}^T \boldsymbol{\sigma}(\mathbf{u}) \hat{\mathbf{n}} dS + \int_{\partial\Omega_N} \mathbf{v}^T \mathbf{h} dS.$$

With the boundary condition $\mathbf{u} = \mathbf{g}$ on $\partial\Omega_D$, we can further write this as

$$(2.9) \quad \int_{\Omega} \boldsymbol{\varepsilon}(\mathbf{v})^T C \boldsymbol{\varepsilon}(\mathbf{u}) dA = \int_{\Omega} \mathbf{f}^T \mathbf{v} dA + \int_{\partial\Omega_D} \mathbf{v}^T \boldsymbol{\sigma}(\mathbf{g}) \hat{\mathbf{n}} dS + \int_{\partial\Omega_N} \mathbf{v}^T \mathbf{h} dS$$

and the right hand side is now independent of \mathbf{u} . Since \mathbf{v} was an arbitrary test function, this equation holds for all v in a suitable Hilbert space X also containing \mathbf{u} .

For equation (2.9) to be well defined, we need to ensure that each of the integrals do not diverge.

The integrals on the right hand side are integrals of dot products of \mathbf{v} and functions defining the problem. As shown in section 2.2 of the attached report for the first part of the project, these are all finite if $\mathbf{v} \in H^1(\Omega)$ and $\mathbf{f}, \boldsymbol{\sigma}(\mathbf{g}), \mathbf{h} \in L^2(\partial\Omega)$ componentwise. In the problems we solve in this report, $\mathbf{f}, \boldsymbol{\sigma}(\mathbf{g}), \mathbf{h} \in L^2(\partial\Omega)$ holds.

The integral on the left hand side is a sum of integrals on the form

$$\int_{\Omega} c \frac{\partial}{\partial \gamma} v_{\alpha} \frac{\partial}{\partial \delta} u_{\beta} dA,$$

where $\alpha, \beta, \gamma, \delta$ are either x or y . By the Cauchy-Schwartz inequality, these are all finite when $\mathbf{u}, \mathbf{v} \in H^1(\Omega)$ componentwise.

We can now conclude that the integral equation (2.9) is well defined when we choose

$$X = H^1(\Omega) \times H^1(\Omega).$$

We now state the variational form of our problem as

Find $\mathbf{u} \in X$ such that $a(\mathbf{u}, \mathbf{v}) = l(\mathbf{v}), \forall \mathbf{v} \in X$

$$(2.10) \quad a(\mathbf{w}, \mathbf{v}) = \int_{\Omega} \boldsymbol{\varepsilon}(\mathbf{v})^T C \boldsymbol{\varepsilon}(\mathbf{w}) dA$$

$$l(\mathbf{v}) = \int_{\Omega} \mathbf{f}^T \mathbf{v} dA + \int_{\partial\Omega_D} \mathbf{v}^T \boldsymbol{\sigma}(\mathbf{g}) \hat{\mathbf{n}} dS + \int_{\partial\Omega_N} \mathbf{v}^T \mathbf{h} dS$$

2.4. Discretization. In order to solve the above variational problem using the Finite element Galerkin projection method, we use triangular finite elements with linear polynomial basis functions in each component for our vector functions. On our reference triangle T_{ref} with vertices $\{\mathbf{p}_0 = [0, 0], \mathbf{p}_1 = [1, 0], \mathbf{p}_2 = [0, 1]\}$ we thus have 6 degrees of freedom, characterised by the coefficients of our vector basis functions

$$(2.11) \quad \hat{\phi}_{i,d} = [(1-d)\hat{\phi}_i, d\hat{\phi}_i], \quad d \in \{0, 1\}, i \in \{0, 1, 2\},$$

where $\hat{\phi}_i$ are the standard linear polynomial basis functions determined by the dual space functionals

$$(2.12) \quad \{N_i \mid N_i(\mathbf{p}_j) = \delta_i^j, i, j \in \{0, 1, 2\}\}.$$

As a linear index of our global basis functions we use ϕ_n , $n \in \{0, \dots, N-1\}$, where the mapping from the nodal index and vector component is $n(j, d) = 2j + d$ with $j \in \{0, \dots, M-1\}$ being the nodal indices. With this basis, we can write our finite element solution u_h as $\sum_{n=0}^{N-1} U_{h,n} \phi_n$, where \mathbf{U}_h is a column vector of N entries.

Given that equation (2.10) needs to hold for all all ϕ_n as test functions, we have the equations

$$\begin{aligned} a(\mathbf{U}_h, \phi_n) &= l(\phi_n), \forall n = 0, \dots, N-1 \\ \sum_{k=0}^{N-1} U_{h,k} a(\phi_k, \phi_n) &= l(\phi_n), \forall n = 0, \dots, N-1 \\ [a(\phi_0, \phi_n) &\quad \cdots \quad a(\phi_{N-1}, \phi_n)] \mathbf{U}_h = l(\phi_n), \forall n = 0, \dots, N-1. \end{aligned}$$

We can now define the matrix A_h and vector \mathbf{f} as

$$A_h = [A_{ij}]_{i,j=0}^{N-1} = [a(\phi_j, \phi_i)]_{i,j=0}^{N-1} \quad \mathbf{f} = [f_i]_{i=0}^{N-1} = [l(\phi_i)]_{i=0}^{N-1}$$

and the system reduces to the matrix equation

$$(2.13) \quad A_h \mathbf{U}_h = \mathbf{f}.$$

2.5. Periodic Solutions. In order to search for periodic solutions of our governing equation (2.2) without any forcing term f , we apply the ansatz $\mathbf{u}(t, x, y) = \mathbf{u}(x, y)e^{\omega t}$, leading to the eigenvalue problem

$$(2.14) \quad \rho\omega^2 \mathbf{u}(x, u) = \nabla \boldsymbol{\sigma}(\mathbf{u}).$$

When we discretize this problem in space by the Finite Element Galerkin approach as above, we arrive at the generalised eigenvalue problem

$$(2.15) \quad \omega^2 \rho M_h \mathbf{U}_h = A_h \mathbf{U}_h,$$

where $M_h \in \mathbb{R}^{N,N}$ is the mass matrix of our basis functions, defined by

$$(2.16) \quad (M_h)_{i,j} = \int_{\Omega} \phi_i^T \phi_j d\Omega, \quad i, j \in \{0, \dots, N-1\}.$$

3. IMPLEMENTATION

3.1. Convergence in the L^2 norm. In order to verify that our solver is producing accurate results, we attempt to solve a problem with a known analytical solution. To this end, we choose the problem

$$\begin{aligned} \nabla^T \boldsymbol{\sigma}(u) &= -\mathbf{f} = -[f_1, f_2] \quad \text{in } \Omega = [-1, 1]^2, \quad \mathbf{u} = 0 \quad \text{on } \partial\Omega, \\ f_1 &= \frac{E}{1-\nu^2} (-2y^2 - (1-\nu)x^2 - 2xy(1+\nu) + 3 - \nu), \\ f_2 &= \frac{E}{1-\nu^2} (-2x^2 - (1-\nu)y^2 - 2xy(1+\nu) + 3 - \nu). \end{aligned}$$

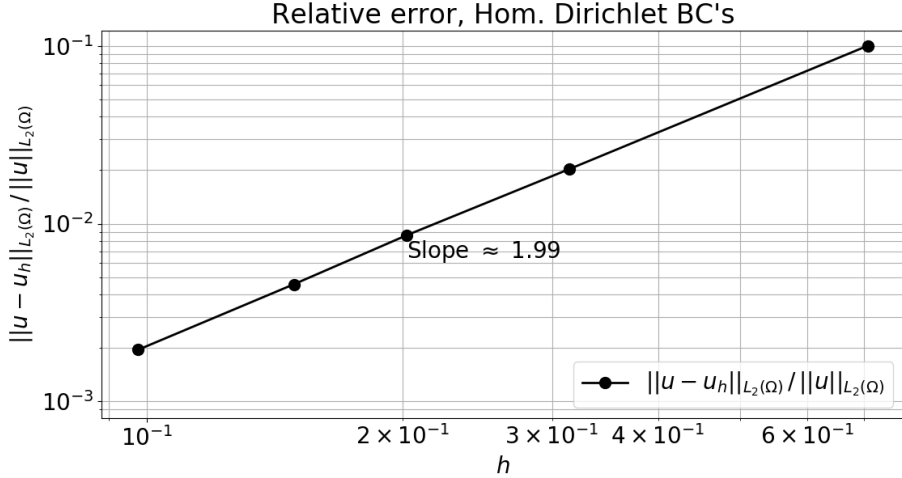


FIGURE 1. Relative error in the $L^2(\Omega)$ norm between our FEM solution \mathbf{u}_h and the exact solution \mathbf{u} plotted on a log-log scale versus a characteristic element size h . In our case, h is chosen as the maximum triangle side length in our triangulation, and slope of the line indicates second order convergence in the $L^2(\Omega)$ norm.

This problem has the analytical solution

$$(3.1) \quad \mathbf{u}(x, y) = [(1 - x^2)(1 - y^2), (1 - x^2)(1 - y^2)],$$

as is verified by the code in appendix A. In order to solve this problem with our FEM solver we choose the underlying function space

$$X = H_0^1(\Omega) \times H_0^1(\Omega).$$

Solving the above problem for a finer and finer grid with our `Elasticity2DSolver()` class, we find second order convergence in the $L^2(\Omega)$ norm between our FEM solution \mathbf{u}_h and the analytical solution \mathbf{u} . This second order convergence is illustrated in figure 1.

We have good reason to believe a second order convergence is to be expected. The problem we solve in this report is similar to the two dimensional Poisson problem we solved in the first part of the project and the finite element method we use in this report is based on the method developed for the Poisson problem. In the report for the first part of the project we showed that our element method has second order convergence under reasonable assumptions on the smoothness of the solution, source term and boundary conditions. These assumptions are that the source term, f , and Neumann boundary term, g , are both L^2 on Ω and that the solution $u \in H^2(\Omega)$, assumptions that are satisfied for our constructed problem.

The main goal of this report is however to solve for vibration frequencies and modes of 2D plates made of different kinds of materials. This problem reduces down to an analytical eigenvalue problem as seen in equation (2.14). In order to solve the large, sparse, generalized eigenvalue problem in equation (2.15), we make use of the `eigsh()` function from the `scipy.sparse.linalg` package [1].

4. NUMERICAL EXPERIMENTS

When we solve equation (2.15) for the k 'th mode vibration frequency ω_k and displacement coefficients $\mathbf{U}_{h,k}$, we wish to display both the resulting grid when displacements of each element is included, and the stresses induced on our domain by this displacement. As we are using linear polynomials as our basis functions on each element, and the elements of $\boldsymbol{\sigma}(\mathbf{u})$ only depends on derivatives of the displacement field, we end up with a constant contribution from each basis function to the stress matrix in each element. As a simple heuristic for calculating the stress matrix in each element, we simply average the calculated stress matrix from each of the basis functions on our element.

When we wish to visualize these stresses on a surface however, we cannot display the stress matrix directly. In order to colour our elements we need a scalar measurement of stress, and to this end we compute the mean total stress (MTS) in each element. This MTS is the average of the eigenvalues of the stress matrix, and knowing that the trace of a matrix equals the sum of the eigenvalues of that matrix, we calculate $\text{MTS}(\boldsymbol{\sigma})$ at element K as

$$(4.1) \quad \text{MTS}(\boldsymbol{\sigma}_K) = \frac{\sigma_{K,xx} + \sigma_{K,yy}}{2}.$$

To test our linear elasticity solver on models of some real world materials, we find the natural vibrations of idealised $1\text{ m} \times 1\text{ m}$ -plates in three common materials. Aluminium, stainless steel and timber, for which the mechanical properties of are found in reference tables and are reproduced in table 2. And in order to better visualize these displacements, we animate the grid triangulation with displacement $\mathbf{u}_k(t) = \sin(t)\mathbf{U}_{h,k}$.

Animations of the vibration modes 3, 6, 7, and 9 for the three plates with a triangulation on a grid of 60×60 nodes are found in the attached animation folder.

	Youngs Modulus [GPa]	Poisson's Ratio	Density [kg/m^2]
Aluminum, 6061-T6:	69	0.35	270
Stainless Steel, 18-8:	193	0.305	793
Timber, western Larch:	12.9	0.276	5.2

TABLE 2. Material properties of our test materials. The density per area is given for a flat, 1 cm thick material. Material properties are sourced from [2, Stainless Steel], [3, Timber], [4, Aluminium] and [5, Aluminium, Steel], and [6, Timber].

To give an impression of what our animations show, a half cycle of the vibrational modes 3 and 7 for each of the materials Stainless Steel, Aluminium and Timber are presented in figures 2a, 2b, 2c, 2d, 2e, and 2f, respectively.

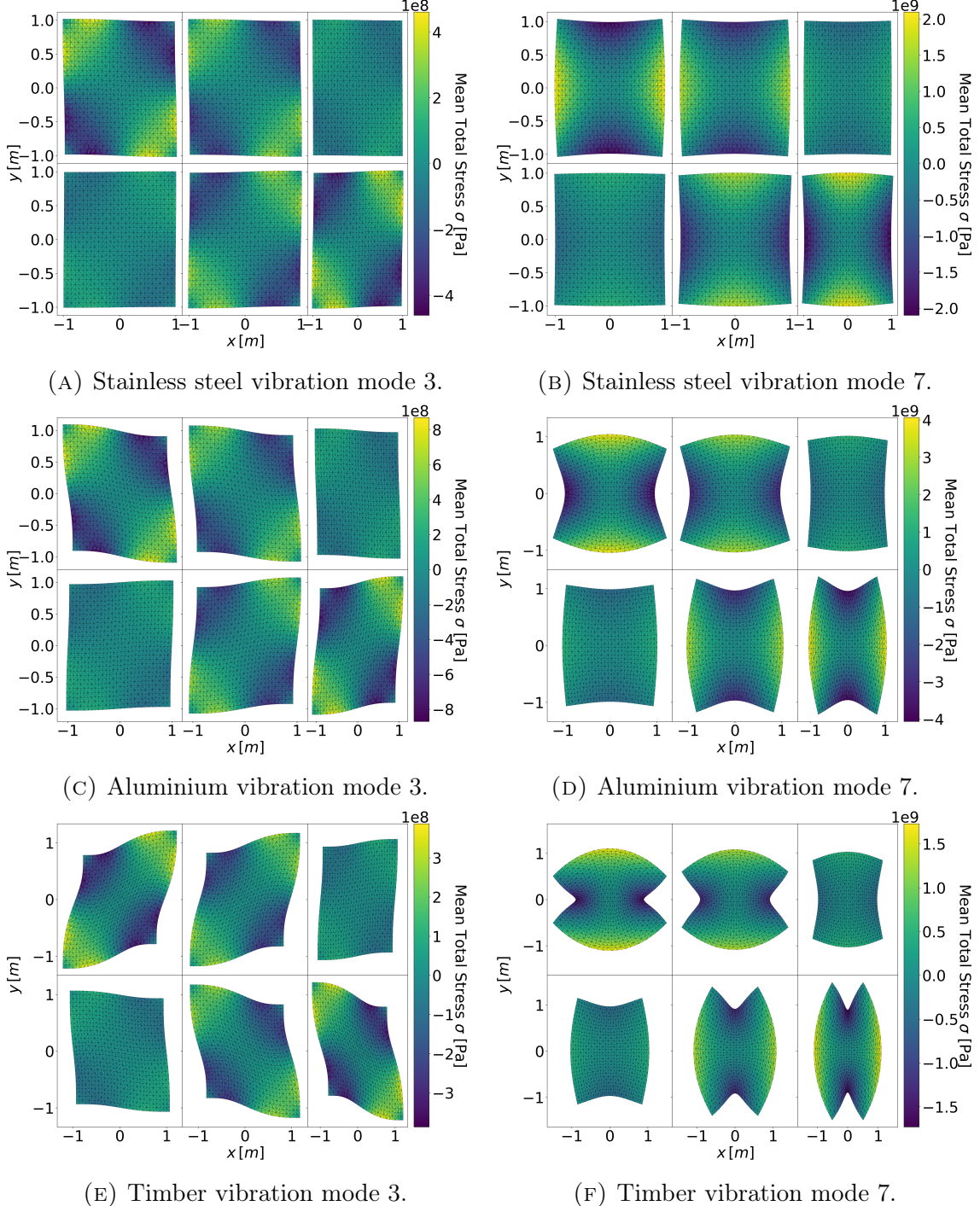


FIGURE 2. Comparison of the vibration modes for the three materials, stainless steel, aluminium and timber, at vibration mode 3 and 7. Material properties for each material is taken from table 2. Each solution uses 1682 elements with 60^2 nodes.

4.1. Vibration frequencies. The frequencies of the free vibrations of the $1\text{ m} \times 1\text{ m}$ plates are shown in figure 3 along with the proportions to the fundamental frequency of the plates. The vibration frequencies are distributed nearly proportionally to

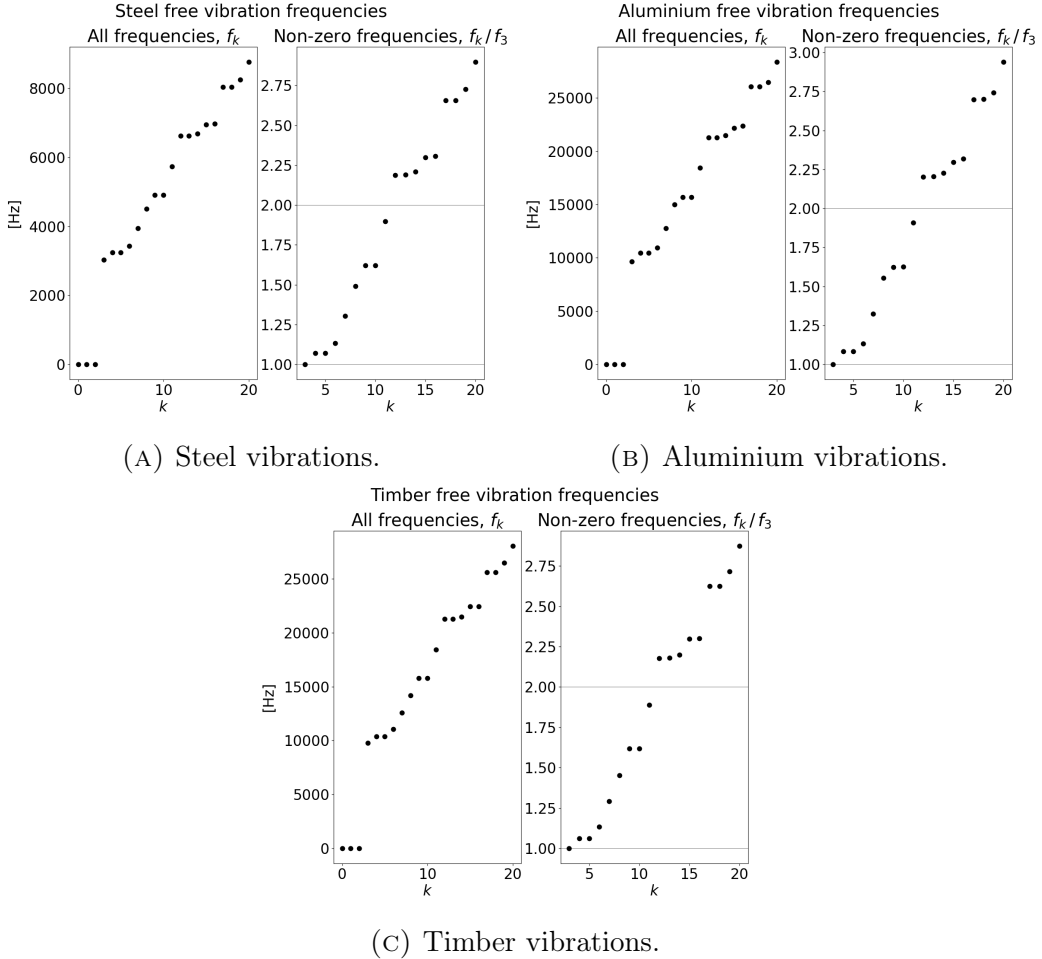


FIGURE 3. Vibrations.

each other and since no non-zero vibrations are integer multiples of the fundamental frequency, no plates experience harmonic frequencies.

5. DISCUSSION

Figures 2a, 2c and 2e shows vibration mode 3 for each of the materials. We see that timber is more deformed than the other two materials, with steel being the least deformed. This agrees with that the Young's modulus of steel is greatest, while timber has the lowest Young's modulus. Although the amplitude of deflection is different for each material in their first non-zero vibrational frequency mode, the general shape of deflection appears qualitatively to be similar. The fact that this first proper vibrational mode is quite similar for each type of material is not very surprising given that the underlying geometry for each material is identical. To better compare the shapes of the vibrational modes between materials, we could have scaled the deflections to have the same maximal values before visualizing them. This would however not communicate the different vibration response for each material due to their properties like density, Young's modulus and Poisson's ratio.

From the attached animations we see that vibration mode 6 differ from all the other vibration modes in that the stress does not appear to be continuous across the

plate. This could be due to the way we decide the colour for each triangle in our mesh.

Figure 2 shows vibration modes 3 and 7 for all three materials. In vibration mode 7 the materials are stretched in a different manner than in mode 3, but the amplitude of deflection is still greater for timber than the two other materials, while steel has the smallest.

Regarding harmonic frequencies we see from figure 3 that none of the overtones, f_k , are multiples of the natural frequency, f_3 . The frequencies f_{11} and f_{20} for all three materials are close with relative frequencies of $\frac{f_{11}}{f_3} \approx 1.9$ and $\frac{f_{20}}{f_3} \approx 2.9$ respectively.

Figure 3 also shows that the frequencies of aluminium and timber only differ slightly. This result is surprising since the Young's modulus and density are much lower for timber than aluminium, but it could be that the differences in Young's modulus and density cancel each other out. Alternatively, it could be the case that with constant density, Young's modulus and Poisson's ratio, the vibrations are proportional to a function of the triangulation.

We did not obtain any vibrations from mode 0, 1 or 2, but this is as expected, according to professor Trond Kvamsdal [7].

Less naive methods of determining the stress over each element could also bring more accurate results. In our work we measure the stress over each element as the mean total stress, using only the gradients on the given element. As we are using linear basis functions, these gradients are discontinuous over element boundaries, so the measured stress across the domain is discontinuous, which is non-physical in uniform plates. An extreme example of this is found in vibration mode 6. More sophisticated methods of calculating the stresses, for example by using patch gradient recovery operators, would be interesting to investigate for this.

Other interesting avenues of further investigation are the effects of non-uniform materials. In construction, concrete is often reinforced with steel bars, making the resulting material stronger, but also non-uniform. Calculations on the vibrations of non-uniform plates, or plates of different geometry, as well as the distribution of frequencies can be quite interesting to consider.

6. CONCLUSION

Solving the linear elasticity equation by means of linear finite elements is found to be feasible in two dimensions on square domain. The free vibrations given by the discretized linear elasticity equation on uniform plates are found to be largely qualitatively equivalent, differing only in scale.

We observe interesting vibrational modes for the square domain in question, seemingly with higher spatial frequency in their oscillations as the vibrational frequency goes up as well. We do not however seem to find any harmonic relationship between higher vibrational frequencies f_k and the first non-zero vibrational frequency f_3 of the type $f_k = n \cdot f_3$, $n \in \mathbb{N}$.

REFERENCES

- [1] Pauli Virtanen et al. “SciPy 1.0: Fundamental Algorithms for Scientific Computing in Python”. In: *Nature Methods* 17 (2020), pp. 261–272. DOI: 10.1038/s41592-019-0686-2.
- [2] World Material. *18/8 Stainless Steel Properties, Yield Strength, Composition, Density, Tensile Strength, Hardness*. 2020. URL: <https://www.theworldmaterial.com/what-is-18-8-stainless-steel/> (visited on 11/06/2020).
- [3] David W. Green, Jerrold E. Winandy, and David E. Kretschmann. “Mechanical Properties of Wood/David W. Green, Jerrold E. Winandy, David E. Kretschmann”. In: *Wood handbook.-Madison, WI: US Department of Agriculture, Forest Service, Products Laboratory* (1999), pp. 4–1.
- [4] World Material. *AL 6061-T6 Aluminum Alloy Properties, Density, Tensile & Yield Strength, Thermal Conductivity, Modulus of Elasticity, Welding*. 2020. URL: <https://www.theworldmaterial.com/al-6061-t6-aluminum-alloy/> (visited on 11/06/2020).
- [5] Engineering ToolBox. *Poisson's ratio*. 2008. URL: https://www.engineeringtoolbox.com/poissons-ratio-d_1224.html (visited on 11/06/2020).
- [6] Engineering ToolBox. *Wood, Panel and Structural Timber Products - Mechanical Properties*. 2011. URL: https://www.engineeringtoolbox.com/timber-mechanical-properties-d_1789.html (visited on 11/06/2020).
- [7] Trond Kvamsdal. *NTNU Professor Trond Kvamsdal*. 2020. URL: <https://www.ntnu.edu/employees/trondkv> (visited on 11/20/2020).

APPENDIX

A: Verify Analytical Solution. Here we use the Computer Algebra System (CAS) `sympy` in Python, to verify that the function

$$(6.1) \quad u(x, y) = [(1 - x^2)(1 - y^2), (1 - x^2)(1 - y^2)]$$

is indeed the analytical solution to the problem in equation ??

```
import sympy as sy
```

```
# Coordinates and function components:
x, y, u1, u2 = sy.symbols("x, y, u1, u2")

# Material properties:
E, nu = sy.symbols("E, nu")

# Analytical solution:
u1 = (x**2 - 1)*(y**2 - 1)
u2 = (x**2 - 1)*(y**2 - 1)

# Strain components:
eps_xx, eps_yy, eps_xy = sy.diff(u1, x), sy.diff(u2, y),
                           sy.diff(u1, y) + sy.diff(u2, x)
eps_vec = sy.Matrix([eps_xx, eps_yy, eps_xy])
```

```

# Stress-Strain Transformation:
C = (E/(1 - nu**2))*sy.Matrix([[1, nu, 0], [nu, 1, 0], [0, 0,
(1 - nu)/2]])

# Stress components:
sigma_xx, sigma_yy, sigma_xy = C @ eps_vec

# Nabla times Stress matrix:
grad_sigma = sy.Matrix([sy.diff(sigma_xx, x) + sy.diff(
sigma_xy, y),
sy.diff(sigma_xy, x) + sy.diff(
sigma_yy, y)])

# Analytical Source term:
f_1 = (E/(1 - nu**2))*(-2*y**2 - x**2 + nu*x**2 - 2*nu*x*y - 2*
x*y + 3 - nu)
f_2 = (E/(1 - nu**2))*(-2*x**2 - y**2 + nu*y**2 - 2*nu*x*y - 2*
x*y + 3 - nu)
f_vec = sy.Matrix([f_1, f_2])

components_equal = sy.simplify(grad_sigma + f_vec).equals(sy.
Matrix([0, 0]))

if components_equal:
    print(f"The equation Nabla^T sigma(u) = -f has an
analytical solution:")
    print("\ntu(x, y) = [(x^2 - 1)(y^2 - 1), (x^2 - 1)(y^2 -
1)]")
    print("given source vector f(x, y) = [f_1, f_2]:")
    print(f"\n\ntf_1 = {sy.simplify(f_1)},\n\ntf_2 = {sy.simplify(
(f_1).")})

```

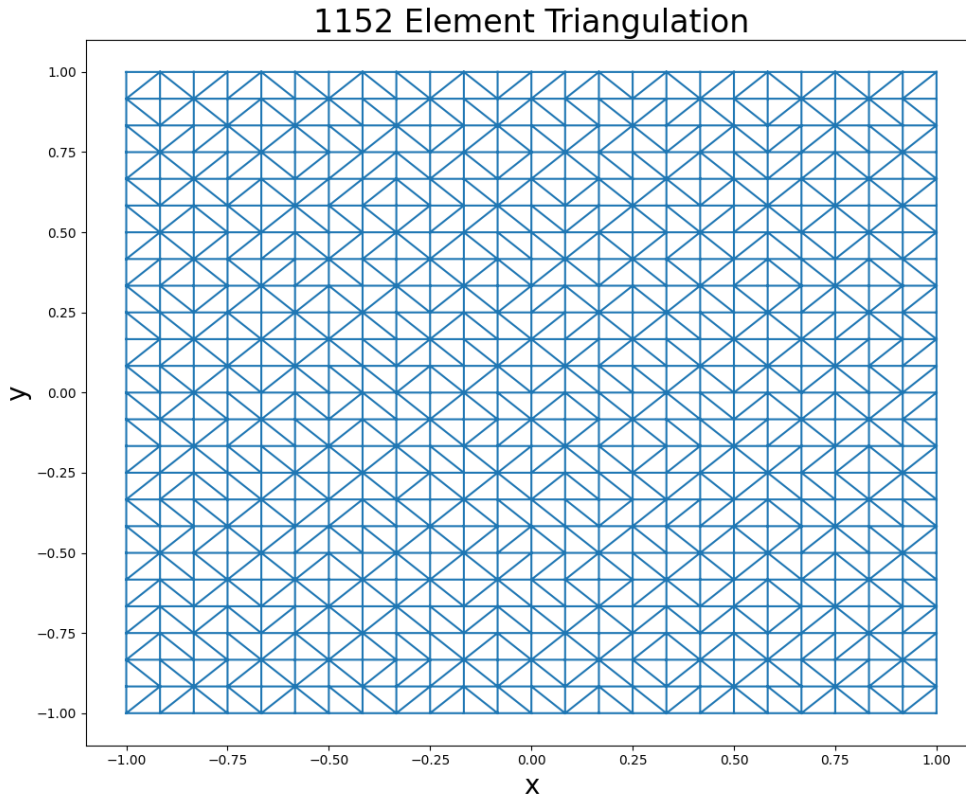


FIGURE 4. Semi Uniform Triangulation of the domain $\Omega = [-1, 1]^2 \subset \mathbb{R}^2$. All triangles are of close to equal size, but with different orientations across the domain.

B: Plate Triangulation. To illustrate the triangulation used when performing our Finite Element analysis, we show figure 4.